The Journal of Veterinary Medical Science

FULL PAPER

Internal Medicine

Optimal placement of the region of interest for bolus tracking on brain computed tomography angiography in Beagle dogs

Sieun PARK[1)], Min JANG[2)], Kija LEE[2)], Hojung CHOI[3)], Youngwon LEE[3)], Inchul PARK[1)] and Sooyoung CHOI[1)]*

[1)]College of Veterinary Medicine, Kangwon National University, 1 Kangwondaehak-gil, Chuncheon 24341, Republic of Korea
[2)]College of Veterinary Medicine, Kyungpook National University, 80 Daehak-ro, Daegu 41566, Republic of Korea
[3)]College of Veterinary Medicine, Chungnam National University, 99 Daehak-ro, Daejeon 34134, Republic of Korea

ABSTRACT. This study aimed to determine the optimal placement of the region of interest (ROI) among four anatomical sites—pulmonary artery (PA), pulmonary vein (PV), aortic arch (AA), and carotid artery (CA)—in computed tomography (CT) brain angiography with automatic bolus tracking in healthy beagle dogs. Six beagles were included, and CT brain angiography was performed four times for each dog, to cover each ROI. The scan parameters, amount, and injection rate of the contrast medium were the same. The major intracranial arteries were selected for quantitative and qualitative evaluation: caudal cerebellar artery (CcA), basilar artery (BA), rostral cerebellar artery (RcA), caudal cerebral artery (CCA), middle cerebral artery (MCA), and rostral cerebral artery (RCA). Quantitative evaluation showed significantly higher CT attenuation values for the RcA, CCA, and MCA in the PA group and RcA and MCA in the PV group than in the CA group. Qualitative analysis revealed significantly higher scores for the BA, CCA, and MCA in the PA and PV groups than in the CA group. Venous contamination did not differ significantly among the ROIs, but the mean scores of the AA and CA groups were higher than those of the PA and PV groups. CT brain angiography using bolus tracking in the beagle dogs showed that the ROI should be placed at the PA or PV rather than at the CA for optimal images with strong contrast enhancement of the BA, RcA, CCA, and MCA and minimal venous contamination.

KEY WORDS: bolus tracking, brain angiography, computed tomography, dog, region of interest placement

J. Vet. Med. Sci.
83(8): 1196–1201, 2021
doi: 10.1292/jvms.20-0724

Received: 21 December 2020
Accepted: 26 May 2021
Advanced Epub:
22 June 2021

Computed tomography angiography (CTA) can be used to visualize the intracranial vessels; thin-slice continuous images of the vessels can be obtained using iodine-based contrast material. In human medicine, this modality is used to diagnose and evaluate vascular diseases, including intracranial aneurysms, arteriovenous malformations, dural arteriovenous fistulas, and intracranial arterial steno-occlusive disease [21, 28]. Magnetic resonance angiography (MRA) relies on the intrinsic magnetic properties of body tissues and blood without the use of ionizing radiation or contrast agents [10]. CTA, on the other hand, has fewer motion artifacts than magnetic resonance imaging; it provides highly sensitive images, and its scan duration is shorter with newer scanners [20, 21].

The administration of an intravenous contrast medium is essential for CTA. The available methods of CTA include fixed-scan delay, the test-bolus technique, and bolus tracking. Optimal scan protocols have been determined for these methods [2, 19, 22]. The fixed-scan delay method is used to examine the intracranial arterial phase without considering the differences in contrast-agent transit time, while the test-bolus technique is used to measure the time from the initiation to the arrival of the contrast agent. Bolus tracking is used to monitor the contrast medium dynamics within the region of interest (ROI) in real-time to obtain optimal contrast-enhanced images. To trigger a scan, the ROI should be placed in the desired vessel, and the predetermined computed tomography (CT) attenuation value (Hounsfield unit [HU]) of the ROI set to initiate the scan automatically. In human studies, the ROI for CT brain angiography has been placed in the anterior aortic arch, internal carotid artery, or distal common carotid artery [12]; ROI placement has been a subject of study for obtaining CTA images with optimal brain arterial opacification [12, 29]. However, veterinary research on the placement of the ROI for brain angiography is lacking.

*Correspondence to: Choi,S.: choisooyoung@kangwon.ac.kr

Five pairs of the main arteries—caudal cerebellar artery (CcA), which originates from the basilar artery (BA), rostral cerebellar artery (RcA), caudal cerebral artery (CCA), middle cerebral artery (MCA), and rostral cerebral artery (RCA)—directly supply the brain in dogs. These paired vessels, except CcA, arise from the arterial circle called the circle of Willis. We hypothesized that ROI placement for CTA using bolus tracking would be different from that in human medicine, and good quality CTA by optimal placement of the ROI can facilitate better visualization of the above main arteries. The main purpose of this study was to determine the ideal placement of the ROI for optimal images of the main arteries minimally contaminated by venous structures in beagle dogs obtained with CTA using bolus tracking. Based on the sequential pathway of the intravenous contrast medium, four arteries, including the pulmonary artery (PA), pulmonary vein (PV), aortic arch (AA), and carotid artery (CA), were used as ROIs.

MATERIALS AND METHODS

All experiments were approved by the Kangwon National University Animal Care and Use Committee (KW-180716-1). This study included six healthy 2-year-old male beagle dogs with no history of cerebrovascular disease. Their mean bodyweight was 11.5 ± 1.1 kg (mean ± standard deviation (SD)). Blood tests, urinalysis, radiography, echocardiography, and abdominal ultrasonography were performed before the experiment. These examinations revealed no remarkable findings or underlying diseases, contrary to the purpose of the study.

Four CT scans were performed consistently for each dog with four different ROIs, including the PA, PV, AA, and CA. There was an interval of at least 3 days between the scans. During CT, the heart rates of the dogs were monitored to ensure they remained above 100 beats/min and recorded before premedication, after induction, and before and immediately after a scan.

For the CT scan, midazolam (0.3 mg/kg) was intravenously administered for premedication, and propofol (4 mg/kg) was administered before endotracheal intubation. Anesthesia was maintained with oxygen and isoflurane. The dogs were placed in a sternal recumbency position, and their forelimbs were pulled caudally to maintain a humanoid position. An 18-gauge over-the-needle intravenous catheter was used in the cephalic vein and connected to a contrast injection system (Salient; Imaxeon, Sydney, Australia). A 16-channel multidetector CT unit (Alexion; Canon Medical Systems, Ohtawara, Japan) was used for the cerebral angiography, and a pre-contrast helical scan was performed from the head to the thorax in the rostral-to-caudal direction to determine the position of the bolus-tracking site and CTA. The trigger threshold for bolus tracking was set at 50 HU, plus the mean HU of each ROI. The dose of intravenous iodinated contrast medium (Omnipaque, iohexol, 300 mg iodine/ml; GE Healthcare Ireland, Cork, Ireland) was fixed at 20 ml/dog. The contrast medium was injected at a rate of 4 ml/sec using a contrast injection system, and the contrast injection pressure was recorded. When the HU of the ROI reached the threshold HU after contrast medium injection, CT brain angiography was automatically initiated at the occipital bone level in the caudal-to-rostral direction with a 5-sec delay after the trigger. Breath-holding was maintained during bolus tracking and the CT, and the scan duration was fixed at 10 sec. The parameters for the pre-contrast helical scan and angiography were as follows: 120 kV, 200 mA, rotation time of 0.75 sec/rotation, pitch factor of 0.938, and scan thickness of 0.5 mm. The reconstruction parameters were: slice thickness of 0.5 mm and slice interval of 0.3 mm with the standard algorithm. The proper ROIs for triggering were determined using pre-contrast images. The PA and PV were selected at the T8 level, AA was selected at the heart base level, and CA was selected at the C3 level (Fig. 1). These anatomical landmarks for ROI placement were uniformly applied in all the dogs, as their body shapes were almost identical.

Five main intracranial arteries, including BA, RcA, CCA, MCA, and RCA, were evaluated using a digital viewer (ViewRex; TechHeim Co., Ltd., Seoul, Korea). The image quality of the CcA was not sufficient for the quantitative analysis. The CT attenuation value for each artery was measured using axial images, and round ROIs for the CT attenuation value measurement were as large as possible but not so large as to approach the edges of the artery. To ensure a consistent location for the CT attenuation value measurements, the ROIs were placed within the segment closest to the circle of Willis; these locations were also uniformly applied for qualitative analysis. Contrast enhancement of a pair of arteries (except the BA) was considered the same bilaterally, and all measurements were performed on the left side.

The image volume data were transferred to a special software program (Xelis, Infinitt, Seoul, Korea), and 3D volume rendering (VR) was performed. Before the analysis, we assessed any anatomical variations in the circle of Willis based on a previous study [27] that identified aplasia of the RCA or rostral communicating artery in dogs. Qualitative analysis was conducted using two different volumes of interest (VOI): the cranial fossa for cerebral vessels and the caudal fossa for cerebellar vessels. First, for the simultaneous evaluation of cerebral arteries, including the CCA, MCA, and RCA, and venous contamination, we created VR images with the VOI set to show the cranial fossa. Second, we created VR images with the VOI set to show the caudal fossa without the tentorium osseum to visualize the CcA, RcA, and BA. Arterial enhancement (0=bad, 1=mild, 2=moderate, 3=excellent) and venous contamination (0=none to mild, 1=moderate, 2=remarkable) were scored for the opacification of each vessel (Figs. 2 and 3).

The measured values from 24 series of CT images were analyzed using GraphPad Prism Software (GraphPad Prism version 8; GraphPad Software Inc., San Diego, CA, USA). The Kruskal-Wallis test with Dunn's multiple comparison test was used for the analysis, and *P*-values less than 0.05 were considered statistically significant.

RESULTS

In total, 24 series of CT scans were performed. The mean heart rates before premedication, after induction, and before and immediately after a scan were 112.2 ± 11.5, 130.1 ± 18.8, 120.3 ± 18.0, and 116.8 ± 16.4, respectively. The mean contrast injection pressure was 147.5 ± 3.7 psi. For ROI placement, because the PA and PV are smaller than the AA and more easily affected by

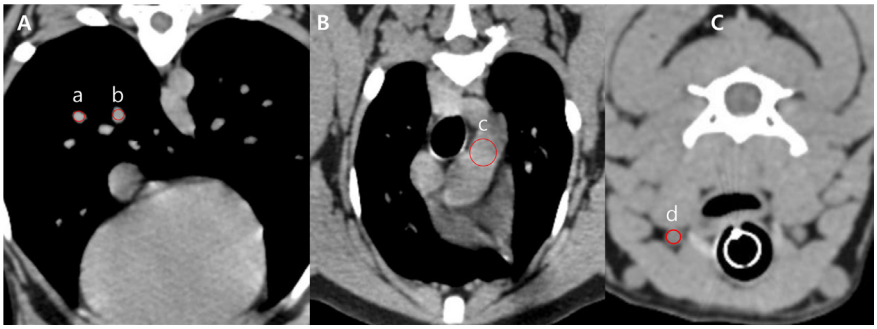

Fig. 1. Region of interest(ROI) placement for triggering in bolus tracking. **A–C**. Red circles represent the positions of four ROIs for bolus tracking. Contrast enhancement of the ROI is monitored, and a helical scan is triggered automatically when the hounsfield unit (HU) of the ROI reaches the preset threshold. **A.** Axial image of the T8 level; **B.** Axial image of the heart base level; **C.** Axial image of the C3 level, a. Pulmonary artery, b. Pulmonary vein, c. Aortic arch, d. Carotid artery.

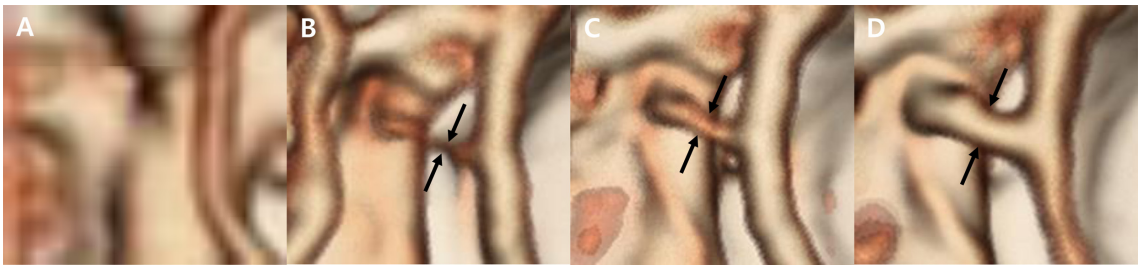

Fig. 2. Qualitative evaluation of the individual artery segments. Three-dimensional volume rendering images were used for qualitative analysis. Each artery was qualitatively evaluated and scored from 0 to 3 as follows: **A.** The vessel is scored as 0 when it is impossible to evaluate the vascular anatomy of the artery (0=bad). **B.** The vessel is scored as 1 when the quality is not sufficient to visualize the vascular anatomy of the artery (1=mild). **C.** The vessel is scored as 2 when it is possible to evaluate the vascular anatomy of the artery but the vessel is not fully enhanced (2=moderate). **D.** The vessel is scored as 3 when the quality is sufficient to evaluate the vascular anatomy of the artery (3=excellent). Pairs of black arrows indicate the middle cerebral artery.

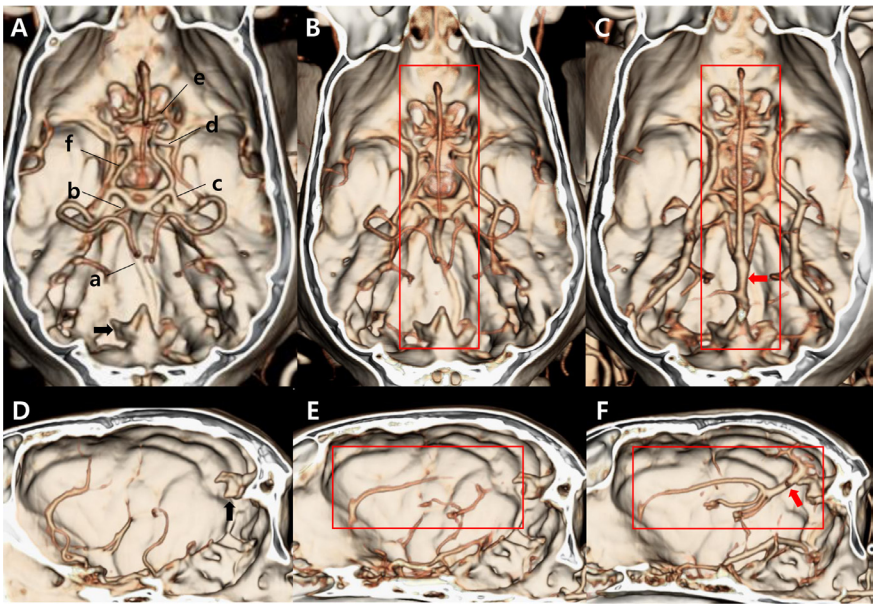

Fig. 3. Qualitative evaluation of venous contamination. **A–C.** Dorsal view of volume rendering images. **D–F.** Left view of volume rendering images. The skull is eliminated until the tentorium osseum (black arrow) is visualized in the dorsal view. We considered the straight sinus (red arrow) and the vessels draining from it (red box) to be representative of venous contamination. Venous contamination is evaluated and scored from 0 to 2 as follows. **A** and **D.** 0=none to mild. When the veins are not or slightly enhanced and do not obscure the arteries, venous contamination is scored as 0. **B** and **E.** 1=moderate. When the veins are visualized slightly and they obscure the arteries, venous contamination is scored as 1. **C** and **F.** 2=remarkable. When the veins are strongly enhanced and they obscure the arteries, venous contamination is scored as 2. a. Basilar artery, b. Rostral cerebellar artery, c. Caudal cerebral artery, d. Middle cerebral artery, e. Rostral cerebral artery, f. Caudal communicating artery.

Table 1. Quantitative analysis of brain arteries (mean ± standard deviation)

Brain artery	CT attenuation values of each group (n=6)			
	PA	PV	AA	CA
BA	310.8 ± 115.4	363.2 ± 80.3*	304.7 ± 84.6	205.3 ± 84.2*
RcA	251.5 ± 60.8*	256.3 ± 20.5$^{\#}$	219.0 ± 42.2	152.7 ± 39.8*,$^{\#}$
CCA	294.3 ± 29.5	264.7 ± 67.8	250.2 ± 88.7	188.0 ± 58.2
MCA	342.2 ± 85.5*	313.8 ± 99.8$^{\#}$	242.3 ± 67.1	149.3 ± 19.7*,$^{\#}$
RCA	357.2 ± 91.7*	246.2 ± 86.9	177.7 ± 43.5	125.0 ± 14.3*

* or $^{\#}$: There was a significant difference between the values with the same superscripts (P<0.05). Computed tomography (CT) attenuation values for the basilar artery (BA), rostral cerebellar artery (RcA), caudal cerebral artery (CCA), middle cerebral artery (MCA), and rostral cerebral artery (RCA) were measured for each region of interest group: pulmonary artery (PA), pulmonary vein (PV), aortic arch (AA), and carotid artery (CA) groups.

Table 2. Qualitative analysis of arterial enhancement and venous contamination (mean ± standard deviation)

Brain vessel	Qualitative score of each group (n=6)			
	PA	PV	AA	CA
CcA	0.5 ± 1.2	1.7 ± 0.8	1.5 ± 0.5	1.3 ± 0.5
BA	2.8 ± 0.4*	2.8 ± 0.4$^{\#}$	2.5 ± 0.5	1.7 ± 0.8*,$^{\#}$
RcA	2.3 ± 1.0	2.5 ± 0.8	1.8 ± 1.5	0.7 ± 0.8
CCA	2.8 ± 0.4*	2.7 ± 0.8$^{\#}$	2.0 ± 1.0	0.7 ± 0.8*,$^{\#}$
MCA	3.0 ± 0.0*	2.7 ± 0.8$^{\#}$	2.0 ± 1.0	0.2 ± 0.4*,$^{\#}$
RCA	2.7 ± 0.8*	2.0 ± 1.0$^{\#}$	0.8 ± 0.7	0.0 ± 0.0*,$^{\#}$
Venous contamination	0.5 ± 1.2	0.5 ± 0.8	1.3 ± 0.5	1.7 ± 0.5

* or $^{\#}$: There was a significant difference between the values with the same superscripts (P<0.05). The scores (from 0 to 3) for the caudal cerebellar artery (CcA), basilar artery (BA), rostral cerebellar artery (RcA), caudal cerebral artery (CCA), middle cerebral artery (MCA), and rostral cerebral artery (RCA) and venous contamination (from 0 to 2) were evaluated for each region of interest group: pulmonary artery (PA), pulmonary vein (PV), aortic arch (AA), and carotid artery (CA) groups.

motion from pulmonary respiration, it was important to maintain breath-holding during bolus tracking. The PA and PV tend to narrow in diameter toward the end of the lobe; therefore, thicker segments of the vascular branch should be selected, if possible (usually located proximally). The CA is also a small artery for ROI placement; however, it is less susceptible to respiratory motion. The diameter of the AA was sufficiently large, meaning that the ROI was easily set and less affected by respiration.

A total of 120 brain arteries were evaluated from four ROI groups: the PA, PV, AA, and CA groups (Table 1). The mean CT attenuation values of the BA and RcA in the PV group were the highest, and they were significantly higher than those in the CA group (P=0.048, P=0.014). The mean RcA attenuation value was significantly higher in the PA group than in the CA group (P=0.037). The mean values of the CCA, MCA, and RCA were highest in the PA group, and the mean values of the MCA in the PA (P=0.004) and PV (P=0.013) groups and the RCA in the PA (P=0.001) group were significantly higher than those in the CA group.

The visualization of the brain arteries and venous contamination was qualitatively scored on 24 VR images (Table 2). The mean scores for the BA, CCA, MCA, and RCA for the PA and PV groups were significantly higher than those for the CA group: PA vs. CA (P=0.05 for BA, P=0.008 for CCA, P=0.001 for MCA, P=0.001 for RCA) and PV vs CA (P=0.05 for BA, P=0.014 for CCA, P=0.007 for MCA, P=0.04 for RCA). No statistically significant difference in venous contamination was found among the ROI groups, but the mean scores of venous contamination were higher for the AA and CA groups than for the other two ROI groups. None of the dogs included in the present study had vascular segment abnormalities.

DISCUSSION

This study aimed to determine the ideal ROI placement for good arterial enhancement with minimal venous attenuation when using bolus tracking for brain angiography in healthy beagle dogs. Four different ROIs (PA, PV, AA, and CA) were selected, and CT scans were obtained four times for each dog. Five pairs of the main arteries supplying the brain (CcA, RcA, CCA, MCA, and RCA) and the basilar artery were analyzed using axial and VR images. Arterial enhancement and venous contamination were assessed quantitatively and qualitatively.

The factors affecting contrast enhancement and scan duration can be divided into three categories: patients, contrast media, and CT scans [2]. To minimize the patient factors, we selected medium-sized 2-year-old male beagles, and breath-holding, disease status, and heart rate were checked and controlled during the experimental period. As none of the dogs had cardiovascular disease, heart rate was considered as indirect evidence of cardiac output, which was one of the major influencing factors in this study. The contrast medium parameters, including iodine mass (concentration, volume) and injection rate, were uniformly applied; therefore, the same magnitude of enhancement was expected. Clinically, the rate of contrast medium injection through a 16-18G catheter in

dogs varies from 3 ml/sec to 5 ml/sec using a power injector system [3]. A faster injection rate shortens the time to vascular arterial enhancement and increases the magnitude of contrast enhancement [4]. However, the pressure of the contrast injection in the power injector increases with the injection rate. One veterinary study on beagle dogs reported the mean psi of the power injector as 198.33 ± 19.83 in 5 ml/sec injection rate groups [15]. We determined that an injection rate of 4 ml/sec was fast enough for contrast enhancement, but not so fast that it would lead to inadequate pressure of contrast injection.

To determine the optimal CT scan protocol, ROI placement was the only variable among the scanning factors in this study. Other scanning factors for bolus tracking, such as scan delay and scan duration, were fixed. In a previous study [7], the mean arrival durations to aortic enhancement appearance and aortic enhancement peak were 7.4 and 12 sec, respectively, when contrast media was injected for 5 sec. Based on this previous study, the scan delay after triggering in this study was fixed at 5 sec so that the aortic enhancement peak time could be included in the scan duration. The 5-sec scan delay was sufficient to cover the preparation time (table movement and interscan time) for the subsequent helical scan. Although a short scan duration should be applied to obtain good-quality CTA images, a 10-sec scan duration using a 0.5 mm slice thickness and 0.938 pitch factor in 16-channel multidetector CT equipment was inevitable. A more advanced CT modality would shorten the scan duration required for high-contrast resolution.

Six arteries (CcA, BA, RcA, CCA, MCA, and RCA) were included for the qualitative assessment, and five arteries (excluding the CcA) were evaluated quantitatively. As part of the initial design of this study, we planned to analyze CcA both qualitatively and quantitatively. However, when using ViewRex software, we found that the diameter of the CcA did not meet the minimum ROI size for attenuation measurement. Thus, they were excluded from the quantitative evaluation. Various human studies have attempted the quantitative assessment of CT angiography, and these studies considered an optimal attenuation value greater than 250 HU [6, 23, 26]. In our study, enhancement in the PA and PV groups was superior to that in the CA group during the quantitative evaluation. The mean attenuation values of all the blood vessels in the PA and PV groups were greater than or equal to 250 HU, whereas the majority in the CA group did not reach 250 HU. This suggests that the PA and PV groups had superior contrast enhancement, they met the contrast enhancement criteria proposed in other studies, and the scan timing of the CA group was too late to involve a peak of contrast enhancement. Usually, approximately 300 HU provides satisfactory 3D images [11]. As the attenuation value reflects 3D reformation, it is logical that the results of our quantitative and qualitative evaluations were similar. The PA and PV groups differed significantly from the CA group based on the qualitative and quantitative assessments. Therefore, both qualitative and quantitative evaluations in this study provided appropriate results for optimal ROI placement.

Venous contamination indicates a shift in the iodine load to the venous bed, resulting in reduced opacification of the arteries. Visualization of the arteries may also be obscured by opacified veins [8]. In our study, the degree of venous contamination was qualitatively assessed using VR images. In human medicine, one study considered the superior sagittal sinus to be representative of the vessels and analyzed artery-vein separation using CT angiography [25]. The study examined both the arterial-dominant and venous-dominant phases based on a total examination duration of 60 sec. We considered the straight sinus and the vessels draining from the straight sinus to be representative of venous contamination (Fig. 3). As such, the scores tended to increase in the AA and CA groups. Because a delayed phase was not included in our study, we could not identify the disappearance of venous contamination, as in the previous human study. Further research on the delayed phase is warranted to understand the full venous-dominant phase of brain angiography in dogs.

In veterinary research, the intracranial vessels of dogs have been assessed using vascular imaging [5, 9, 17, 24, 27, 30]. Ischemic or hemorrhagic strokes, which are referred to as cerebrovascular accidents, have been recognized as a common cause of acute neurologic dysfunction in dogs [1]. MRA has been used for vascular imaging in dogs with strokes, aneurysms, intravascular lymphomas, and cerebral vascular malformations in dogs [18, 30]. In humans, variations in the circle of Willis are commonly found; this increases the possibility of ischemic problems [14, 16], and variations in the circle of Willis in dogs have recently been researched using MRA [27]. Vascular imaging using CTA and MRA would be useful for the evaluation of ischemic problems and intracranial vascular anomalies. However, there are only few published studies on the use of CTA in dogs with stroke and intracranial vascular variations [1], and one report described an intracranial aneurysm in a dog incidentally detected on CTA using a fixed-scan delay (injection-to-scan delay of 10 sec and injection rate of 4 ml/sec) [5]. The CTA protocol using bolus tracking described facilitated the acquisition of good to excellent angiograms of the intracranial arteries.

There are several limitations to our study. First, saline flush could not be administered after contrast-agent injection because we used a single-syringe CT injector for contrast medium only. As a saline flush assists the antegrade movement of the contrast bolus and clears the vascular access site of residual contrast after injection [13], it is particularly beneficial when a small volume of contrast medium is used [2]. Second, because dogs have a relatively short arterial enhancement peak, a shorter CT scan duration is needed for stronger arterial opacification. A shorter scan duration using higher grade CT equipment would result in better image quality of the CcA and small brain arterial branches.

Our findings show that the ROI for triggering should be placed at the PA or PV rather than at the CA for optimal CT brain angiography using bolus tracking, which will facilitate strong arterial attenuation of the BA, RcA, CCA, and MCA and minimal venous contamination in beagle dogs.

CONFLICT OF INTEREST. There are no conflicts of interest to declare.

ACKNOWLEDGMENT. This work was supported by the National Research Foundation of Korea (NRF) grant funded by the Korea government (MSIT) (NRF-2017R1C1B5073755).

REFERENCES

1. Arnold, S. A., Platt, S. R., Gendron, K. P. and West, F. D. 2020. Imaging ischemic and hemorrhagic disease of the brain in dogs. *Front. Vet. Sci.* **7**: 279. [Medline] [CrossRef]
2. Bae, K. T. 2010. Intravenous contrast medium administration and scan timing at CT: considerations and approaches. *Radiology* **256**: 32–61. [Medline] [CrossRef]
3. Bertolini, G. 2010. Acquired portal collateral circulation in the dog and cat. *Vet. Radiol. Ultrasound* **51**: 25–33. [Medline] [CrossRef]
4. Bertolini, G. 2017. Basic principles of MDCT angiography. pp. 37–51. In: Body MDCT in Small Animals: Basic Principles, Technology, and Clinical Applications, 1st ed. (Bertolini, G.), Springer, Cham.
5. Bertolini, G. 2013. Incidental intracranial aneurysm in a dog detected by 16-multidetector row computed tomography angiography. *Case Rep. Vet. Med.* **932746**: 10.1155/2013/932746.
6. Chen, M., Mattar, G. and Abdulkarim, J. A. 2017. Computed tomography pulmonary angiography using a 20% reduction in contrast medium dose delivered in a multiphasic injection. *World J. Radiol.* **9**: 143–147. [Medline] [CrossRef]
7. Choi, S. Y., Lee, I., Seo, J. W., Park, H. Y., Choi, H. J. and Lee, Y. W. 2016. Optimal scan delay depending on contrast material injection duration in abdominal multi-phase computed tomography of pancreas and liver in normal Beagle dogs. *J. Vet. Sci.* **17**: 555–561. [Medline] [CrossRef]
8. Das, K., Biswas, S., Roughley, S., Bhojak, M. and Niven, S. 2014. 3D CT cerebral angiography technique using a 320-detector machine with a time-density curve and low contrast medium volume: comparison with fixed time delay technique. *Clin. Radiol.* **69**: e129–e135. [Medline] [CrossRef]
9. Garosi, L. S. and McConnell, J. F. 2005. Ischaemic stroke in dogs and humans: a comparative review. *J. Small Anim. Pract.* **46**: 521–529. [Medline] [CrossRef]
10. Hartung, M. P., Grist, T. M. and François, C. J. 2011. Magnetic resonance angiography: current status and future directions. *J. Cardiovasc. Magn. Reson.* **13**: 19. [Medline] [CrossRef]
11. Hirai, T., Korogi, Y., Takahashi, M. and Yamashita, Y. 2005. CT angiography in the assessment of intracranial vessels. pp. 55–67. In: Multidetector-row CT Angiography, 1st ed. (Catalano, C. and Passariello, R.), Springer, Berlin.
12. Huang, R. Y., Chai, B. B. and Lee, T. C. 2013. Effect of region-of-interest placement in bolus tracking cerebral computed tomography angiography. *Neuroradiology* **55**: 1183–1188. [Medline] [CrossRef]
13. Indrajit, I. K., Sivasankar, R., D'Souza, J., Pant, R., Negi, R. S., Sahu, S. and Hashim, P. 2015. Pressure injectors for radiologists: A review and what is new. *Indian J. Radiol. Imaging* **25**: 2–10. [Medline] [CrossRef]
14. Jin, Z. N., Dong, W. T., Cai, X. W., Zhang, Z., Zhang, L. T., Gao, F., Kang, X. K., Li, J., Wang, H. N., Gao, N. N., Ning, X. J., Tu, J., Li, F. T., Zhang, J., Jiang, Y. J., Li, N. X., Yang, S. Y., Zhang, J. N., Wang, J. H. and Yang, X. Y. 2016. CTA characteristics of the circle of Willis and intracranial aneurysm in a Chinese crowd with family history of stroke. *BioMed Res. Int.* **2016**: 1743794. [Medline] [CrossRef]
15. Jung, J., Chang, J., Yoon, J. and Choi, M. 2007. CT characteristics of normal canine pulmonary arteries and evaluation of optimal contrast delivery methods in CT pulmonary angiography. *Korean J. Vet. Res.* **47**: 247–254.
16. Kapoor, K., Singh, B. and Dewan, L. I. 2008. Variations in the configuration of the circle of Willis. *Anat. Sci. Int.* **83**: 96–106. [Medline] [CrossRef]
17. Kent, M., Delahunta, A. and Tidwell, A. S. 2001. MR imaging findings in a dog with intravascular lymphoma in the brain. *Vet. Radiol. Ultrasound* **42**: 504–510. [Medline] [CrossRef]
18. Kent, M., Glass, E. N., Haley, A. C., March, P., Rozanski, E. A., Galban, E. M., Bertalan, A. and Platt, S. R. 2014. Ischemic stroke in Greyhounds: 21 cases (2007–2013). *J. Am. Vet. Med. Assoc.* **245**: 113–117. [Medline] [CrossRef]
19. Kerl, J. M., Lehnert, T., Schell, B., Bodelle, B., Beeres, M., Jacobi, V., Vogl, T. J. and Bauer, R. W. 2012. Intravenous contrast material administration at high-pitch dual-source CT pulmonary angiography: test bolus versus bolus-tracking technique. *Eur. J. Radiol.* **81**: 2887–2891. [Medline] [CrossRef]
20. Kim, M. S., Lee, J. W., Kim, S. G. and Kweon, D. C. 2017. Radiation dose and image quality assessment of the bolus timing method for CT angiography. *Iran. J. Radiol.* **14**: e31918 10.5812/iranjradiol.31918.
21. Lin, A., Rawal, S., Agid, R. and Mandell, D. M. 2018. Cerebrovascular imaging: Which test is best? *Neurosurgery* **83**: 5–18. [Medline] [CrossRef]
22. Nakaura, T., Awai, K., Yanaga, Y., Namimoto, T., Utsunomiya, D., Hirai, T., Sugiyama, S., Ogawa, H., Aoyama, M. and Yamashita, Y. 2011. Low-dose contrast protocol using the test bolus technique for 64-detector computed tomography coronary angiography. *Jpn. J. Radiol.* **29**: 457–465. [Medline] [CrossRef]
23. Ramadan, S. U., Kosar, P., Sonmez, I., Karahan, S. and Kosar, U. 2010. Optimisation of contrast medium volume and injection-related factors in CT pulmonary angiography: 64-slice CT study. *Eur. Radiol.* **20**: 2100–2107. [Medline] [CrossRef]
24. Sager, M., Assheuer, J., Trümmler, H. and Moormann, K. 2009. Contrast-enhanced magnetic resonance angiography (CE-MRA) of intra- and extra-cranial vessels in dogs. *Vet. J.* **179**: 92–100. [Medline] [CrossRef]
25. Shirasaka, T., Hiwatashi, A., Yamashita, K., Kondo, M., Hamasaki, H., Shimomiya, Y., Nakamura, Y., Funama, Y. and Honda, H. 2017. Optimal scan timing for artery-vein separation at whole-brain CT angiography using a 320-row MDCT volume scanner. *Br. J. Radiol.* **90**: 20160634 [CrossRef]. [Medline]
26. Tamura, Y., Utsunomiya, D., Sakamoto, T., Hirai, T., Nishiharu, T., Urata, J. and Yamashita, Y. 2010. Reduction of contrast material volume in 3D angiography of the brain using MDCT. *AJR Am. J. Roentgenol.* **195**: 455–458. [Medline] [CrossRef]
27. Tanaka, T., Akiyoshi, H. and Mie, K. 2018. Anatomical variations in the circle of Willis in canines. *Anat. Histol. Embryol.* **47**: 609–612. [Medline] [CrossRef]
28. Wallace, R. C., Karis, J. P., Partovi, S. and Fiorella, D. 2007. Noninvasive imaging of treated cerebral aneurysms, part I: MR angiographic follow-up of coiled aneurysms. *AJNR Am. J. Neuroradiol.* **28**: 1001–1008. [Medline] [CrossRef]
29. Watanabe, Y., Ino, K. and Yoshikawa, K. 2015. Discussion about improvement of stability of the scan timing by placing small ROI in cerebral 3D-CTA. *Open Journal of Radiology* **5**: 224–234. [CrossRef]
30. Wessmann, A., Chandler, K. and Garosi, L. 2009. Ischaemic and haemorrhagic stroke in the dog. *Vet. J.* **180**: 290–303. [Medline] [CrossRef]